Available online at www.sciencedirect.com
SCIENCE DIRECT®
Journal of Power Sources 119–121 (2003) 310–315
JOURNAL OF POWER SOURCES
www.elsevier.com/locate/jpowsour

Vanadia xerogel nanocathodes used in lithium microbatteries

Christina Dewan, Dale Teeters*

Department of Chemistry and Biochemistry, The University of Tulsa, 600 S. College Avenue, Tulsa, OK 74104-3189, USA

Abstract

Microbatteries with nanoscale features were made. Alumina filtration membranes having pores 200 nm in diameter served as the "jackets" to hold a PEO–lithium triflate electrolyte. Graphite particles approximately 75 μm in diameter were placed on the membrane covering numerous electrolyte-filled pores. The bottom of the pores were filled with V_2O_5 xerogel making cathode structures having a circular surface area with a diameter of 200 nm. In some cases, the V_2O_5 xerogel was filled with 35% carbon nanotubes making a nanocomposite cathode material that exhibited better performance. In effect, microbatteries of numerous parallel nanocells were made. These microbatteries were charged and discharged and, though they had low capacities ranging from 3 to 18 mAh/g, it was shown that these small lithium batteries could function in a viable manner.

Keywords: Microbatteries; Nanobatteries; Nanocathodes; V_2O_5 xerogels; Carbon nanotubes

1. Introduction

Microelectromechanical systems (MEMS) and their proposed smaller counterparts nanoelectromechanical systems (NEMS) have great commercial importance in micro- and nanoscale motors, pumps, relays and other components. However, for these minute systems to be fully utilized, they need self-contained power sources. One potential source of energy that has received relatively little attention on the micro- and nanometer scales is the lithium battery. It is an excellent possibility, a miniaturized lithium system can fill this need.

Many articles on microbatteries have appeared in the literature, with thin-film rechargeable batteries with active layers of 1–10 μm being of interest since the 1980s. More recent work includes such studies as those done by Bates et al. where thin-film microbatteries were made by a deposition technique using a metallic lithium electrode layer with a solid Li_3PO_4 electrolyte [1]. Salmon et al. [2] developed a microbattery using a Ni/Zn electrode coupled with an aqueous KOH electrolyte. Fabrication involved a deposition process for the two electrodes, with a polymer layer that is later removed to form the electrolyte cavity. These planar microbatteries were 200 μm × 200 μm and had capacities of 200–300 mC/cm^2 at current densities of 10–20 mA/cm^2 at an operating voltage of 1.5 V. Kinoshita et al. [3] have discussed the conceptual design for a carbon-based rechargeable lithium microbattery and discussed the progress in fabricating the electrode microstructure. Their technology is based on photoresist methods commonly used in the semiconductor industry, and they proposed making arrays of microelectrodes having diameters as small as 5 μm. In the most recent studies, more attempts have been reported at making not only microbattery but nanobattery components and systems that take advantage of nanoscale technology and assembly. Wright and co-workers [4,5] have made Langmuir–Blodgett films that have ion-conducting layers with the potential to be used as electrolytes in nanobattery systems. Fendler [6] appears to be one of the first to use a layer-by-layer self-assembly to construct an entire battery system. Poly(dimethyl diallyl ammonium chloride), graphite oxide nanoplatelets, and polyethylene oxide were assembled in this manner on indium tin oxide with a lithium wire as a counter electrode resulting in high-energy density rechargeable lithium ion batteries. Systems with 10 self-assembled layers have high specific capacities ranging from 1100 to 1200 mAh/g. Martin and co-workers have made several nanoscale electrode systems using a template synthesis method. Systems composed of $LiMn_2O_4$ [7], SnO_2 [8], TiS_2 [9], sol–gel V_2O_5 materials [10], and carbon tubes [11] have been used to make nanoscale electrode materials. These electrodes typically show higher capacities, lower resistance, and lower susceptibility to slow electron-transfer kinetics than standard electrode configurations.

* Corresponding author. Tel.: +1-918-6313147; fax: +1-918-6313404.
E-mail address: dale-teeters@utulsa.edu (D. Teeters).

0378-7753/03/$ – see front matter © 2003 Elsevier Science B.V. All rights reserved.
doi:10.1016/S0378-7753(03)00165-4

The majority of papers on actual functioning microbatteries describe systems where very thin films of electrolyte material were used to construct the battery, or describe the potential for these films to be used in batteries [12–16]. The actual size of the batteries based on the electrode structure was much greater than the nanometer scale. Work referring to nanoscale batteries is usually concerned with the use of nanosized components in macrosystems. By contrast, the work described here is concerned with the construction of individual micrometer scale batteries containing nanometer scale components including nanoscale cathodes. Vanadia xerogels were used to make nanoscale cathode structures. These cathodes are coupled with a polymeric electrolyte confined in 200 nm pores with graphite particle anodes to make individual batteries, having micro- and nanometer-sized electrodes, that can be charged and discharged. These batteries have potential for commercial utilization in MEMS and NEMS, but also because of their small scale, they provide the opportunity to investigate fundamental properties that cannot be studied on macroscale battery systems. For instance, when a single graphite particle is used as an electrode, fundamental questions concerning lithium intercalation in the graphite can be investigated without the interpretation being complicated by other anode components.

2. Experimental

2.1. Cathodes

One of the major tasks of making the nanobattery system was the construction of the cathode. A nanocoating process similar to that described by Caruso and Antonietti [17] was used to put a V_2O_5 sol–gel onto Whatman Anodisc alumina filtration membranes. Approximately 40% of surface area of the membranes were pores having diameters of either 200 or 100 nm. The membranes were 60 μm thick. One side of the alumina membrane was sealed using Parafilm®. This was done by pressing the membrane on the Parafilm®, where the hand pressure and heat helped to seal the pores with the film. The unsealed side of the membrane (bottom) was nanocoated with 0.01–0.03 ml of a protonated vanadium solution prepared by the method described by Pelletier et al. [18]. A 0.5 cm^3 syringe was used to drop the vanadium solution on the membrane. Because the pores were sealed on one side by the Parafilm®, when the solution was applied the pressure within the pores would not allow the solution to penetrate completely through the membrane. This kept the solution localized close to surface of the pores on the side that it was applied. The liquid V_2O_5 sol–gel solution cured within the membrane pores and on the membrane surface. The sol–gel solvent was removed by evaporation at ambient temperature over several days. The resulting xerogel formed a continuous coating on the membrane and, more importantly, formed small nanocathode structures having diameters of 200 nm or less within the membrane pores. The membrane containing the nanocathodes was silver pasted onto a 0.125 mm thick nickel foil, which served as a current collector. Then the membrane was unsealed by carefully pulling off the Parafilm® after the nickel current collector was attached.

The second type of cathode was made by sealing one side of the membrane as described above. However, in this case, the V_2O_5 xerogel cathode was modified by adding 35 wt.% of single-walled carbon nanotubes (Aldrich, CarboLex AP-grade) to the liquid sol–gel solution. The carbon nanotube/V_2O_5 sol–gel solution was mixed by agitation and nanocoated onto the unsealed side of the membrane, as described above. The rest of the cathode presentation was the same as described previously.

2.2. Electrolyte and anode

The solid electrolyte was made by suspending a wax having a chemical formula best described as H–$(CH_2)_{32}$–$(CH_2$–CH_2–O–$)_{10}$–H (Baker Specialty Polymers) in acetone, and adding lithium triflate (Aldrich) to make an ether oxygen to lithium ratio of 15:1. The wax electrolyte solution was slowly heated to a temperature of 120 °C, the melting temperature of the wax, and the acetone was removed by using the rotary evaporator. The resulting wax electrolyte was nanocoated to the non-vanadiated side of the membrane by melting the electrolyte onto the membrane surface. This was done by placing the membrane and wax in a vacuum oven for approximately 1.5 h at 120 °C. The vacuum removed air within the pores and allowed the molten electrolyte to migrate into the pores and to come in contact with the nanocathode structures already present on the opposite side of the alumina membrane. The electrolyte solidified upon removal from the vacuum oven. The membranes were reheated on a hotplate to remove excess electrolyte and to secure the anodes. The anodes used were graphite particles (Ultra Carbon, ultra "F" purity) having particle sizes ranging from <1 to 100 μm. The surface with the exposed electrolyte was lightly "dusted" with graphite particles. There was enough molten wax remaining on the surface to allow the graphite particles to imbed on top of the membrane. This random dusting process resulted in the graphite particles covering pores filled with solid electrolyte. Because these graphite-covered, electrolyte-filled pores were in contact with the nanocathode structures, microelectrochemical cells were constructed.

2.3. Electrochemical studies

The microcells were charged by using a Digital Instruments Nanoscope IIIa AFM where the cantilever tip was used to make contact with individual graphite particles. The AFM tips were made electrically conducting by sputter coating them with a 100 nm gold layer. Fig. 1 is an optical image showing this experimental configuration. The image

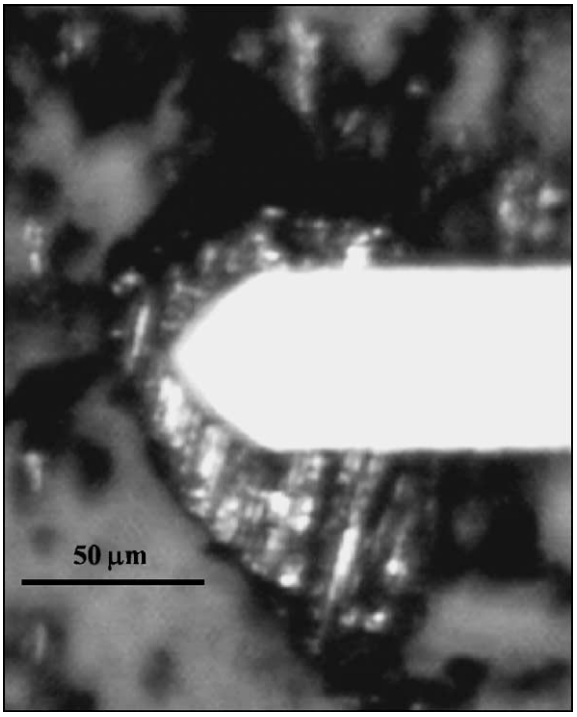

Fig. 1. Optical microscope image of AFM cantilever touching graphite anode particle of microbattery.

shows a cantilever, which is in contact with the graphite particle beneath it. A Digital Instruments signal access module allowed access to electrical contact made with the gold-coated AFM tip touching a graphite particle and the nickel current collector. The purpose of this preliminary work was to construct microbatteries, to develop methods to test them, and to prove that microbatteries with nanocomponents such as nanocathodes could function. In this work, tests of the microbatteries were done open to air under ambient conditions. These conditions certainly reduce battery performance; however, the ability of these small batteries to function could still be tested.

A Keithley model 6430 sub-femtoampere remote source meter was used to conduct charge–discharge cycles. Impedance studies were done on the cathode xerogels to determine electronic conduction and were done using a Hewlett-Packard 4194A Phase/Gain-Phase Analizer over a range of 100 Hz to 40 MHz.

2.4. Imaging and composition studies

The cathodes and membranes were imaged optically by using the optical microscope attached to the Digital Instruments AFM. The surface was also imaged using both the AFM in tapping mode and a Joel JSM-35C scanning electron microscope. Compositions of membrane cross-sections were analyzed using the an energy depressive X-ray spectrometer (EDS) with an accelerating potential of 25 kV and Wineds^{TM} software using a ZAF correction procedure.

3. Results and discussion

It was important to characterize the structure of the nanocathodes in the alumina membrane. Fig. 2a shows the SEM image of the membrane containing only the V_2O_5 xerogel. The membrane has been broken so that the cross-section can be seen and analyzed by the SEM. The bottom layer is the V_2O_5 xerogel, while the striated region above this is the membrane with the fractured pores exposed. Upon careful observation, it can be seen that the V_2O_5 has indeed penetrated the pores of the membrane, and on average, it appears that the V_2O_5 penetrated approximately one fourth of the pore distance. Fig. 3 shows data from the EDS cross-sectional analysis of this membrane. As expected, the very edge at the bottom of the membrane was found to be 94% vanadia by weight. But at approximately 15 μm into the pores, the V_2O_5 content has dropped to a more or less constant level throughout the membrane of

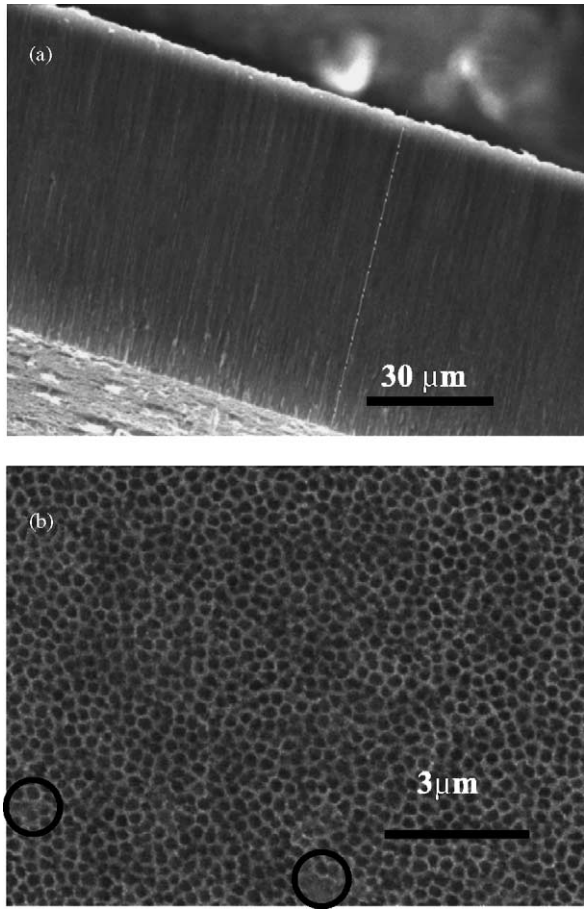

Fig. 2. SEM images of alumina membranes. (a) Cross-section of membrane coated with V_2O_5 xerogel. The striations are the fractured pores in the membrane. The dense layer observed on the bottom is the xerogel. The V_2O_5 xerogel can be seem penetrating approximately 25% of the pore length. (b) Top view of the same membrane showing that most pores remain open after nanocoating with V_2O_5. Circled areas shows region where some V_2O_5 has penetrated the surface.

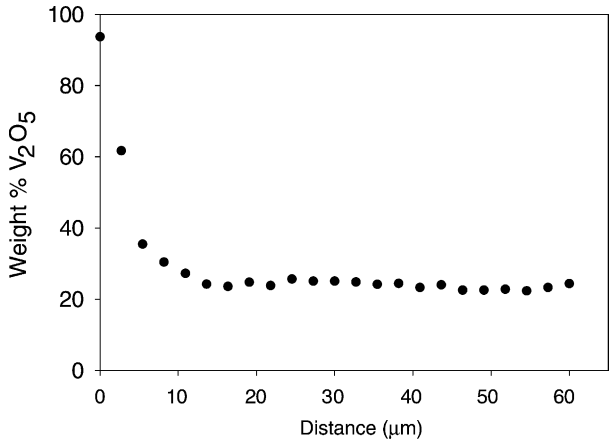

Fig. 3. Graph of the EDS cross-sectional analysis from membrane shown in Fig. 2. The surface nanocoated with V_2O_5 was almost 94% V_2O_5 while further in the pores the V_2O_5 content drops to a constant value of approximately 24%.

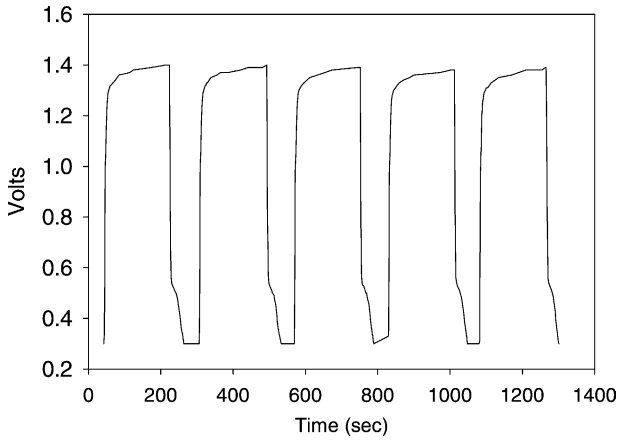

Fig. 4. Charge–discharge data for microbattery having a V_2O_5 cathode without carbon nanotubes.

approximately 24%. This constant level of vanadia throughout the membrane can be attributed to the fact that some of the pores are not sealed well by the Parafilm® and the V_2O_5 sol–gel is able to penetrate all the way through the membrane due to wetting of the alumina surface by the sol–gel and by capillary action. This can be seen in Fig. 2b, which is the SEM of the top of the membrane (side initially sealed with the Parafilm®). As labeled on the image, some pores can be seen that are filled with V_2O_5, though most can be seen to be open and thus not filled. Thus, the average content of the membrane of approximately 24% reflects that some pores are filled with V_2O_5 while most are not filled. The distribution of V_2O_5 shown in Fig. 3 indicates that most of this penetration is only for the first 15 μm or the first quarter of the pore distance.

These cathodes were used to make microcells as described in Section 2.1. In this work, the average size of the graphite particles was approximately 75 μm in diameter, therefore, the batteries will be described as microbatteries. However, similar charging capabilities have been seen in our laboratory for graphite particles less than 1 μm. The AFM tip was brought into contact with a selected graphite anode particle and 50 nA of current was applied for 3 min in order to insert lithium into each V_2O_5 xerogel. The microbattery was subjected to charge–discharge cycles which consisted of charging for 3 min at 50 nA then discharging at a rate of 10 nA to a potential of 0.3 V. Several charge–discharge cycles are shown in Fig. 4. The microbatteries consistently charged to greater than 1.6 V. Several reasons could exist for the low cell potential. As mentioned in Section 2.3, the actual charge–discharge studies were done under atmospheric conditions, which no doubt drastically affects the battery's performance. Low electronic conductivity of the V_2O_5 could also hinder battery performance. Conducting the charge–discharge studies using the AFM system under inert atmosphere conditions will require a special experiment setup and will be done in the future. Since future work will be conducted under inert atmosphere conditions, the issue of electronic conductivity will be addressed here.

Recently, Bachas and co-workers [19] have incorporated carbon nanotubes to enhance electrical properties of sol–gel materials. The addition of carbon nanotubes to the V_2O_5 sol–gel studied here should increase the electronic conductivity in the resulting xerogel composite. Since the cathode structures were of a nanoscale, the addition of nanotubes seems a logical extension of the theme of this research. Impedance data (not shown) collected on thin films of the V_2O_5 xerogel without and with 35% carbon nanotubes demonstrated the improvement in electrical conduction upon the addition of the tubes, with the electronic conductivity increasing by a factor of seven. The batteries were once again charged at 50 nA and consistently charged to slightly greater that 2 V. They were then discharged at a constant current of 10 nA to a potential of 0.3 V. While the tubes may or may not have penetrated into the pores, the addition of the tubes to the V_2O_5 making a composite system did improve battery performance.

A rough approximation of the capacity of these nanobatteries can be made, considering the size of the pores, the depth of penetration of the V_2O_5 into them and the size of the graphite anode particle, which would be the limiting electrode area. The surface area of the graphite particles was determined from the optical pictures such as those shown in Fig. 1. The surface area of the particles used to make the microbatteries ranged from 2.9×10^{-5} to 5.8×10^{-5} cm^2, and since manufacturer's specifications list the pore area to be 40% of the surface area of the membrane, the limiting electrode surface area would be 40% of the graphite particle area. The depth of penetration of the V_2O_5 into the pores can be estimated from Fig. 3, which shows that by approximately 15 μm no additional V_2O_5 enters the pores. For calculation purposes, an average depth of penetration of 5 μm was used and knowing the density of vanadia is 3.35 g/cm^3, the grams of V_2O_5 in the cathode can be calculated.

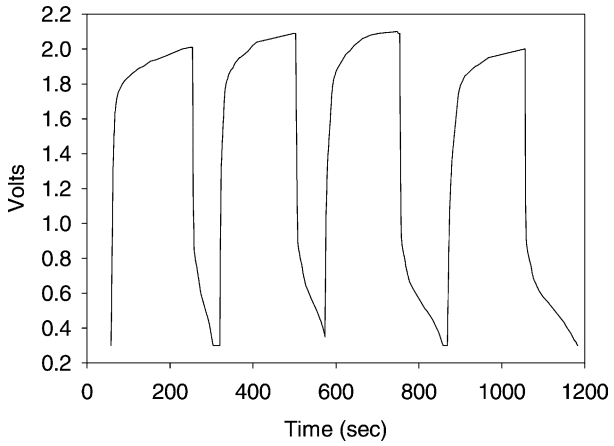

Fig. 5. Charge–discharge data for microbattery having a V_2O_5 cathode with carbon nanotubes.

Using the 10 nA discharge current, the capacities of the microbatteries could be determined.

As inferred in Fig. 4, the capacity of this microbattery without the nanotubes remained relatively constant for each cycle and was calculated to be approximately 3 mAh/g. However, the microbattery with nanotubes increased with each cycle (Fig. 5) with calculated values beginning at 3 mAh/g and reaching 18 mAh/g. It is thus apparent that the addition of the carbon nanotubes, with the increase in electronic conduction, increased the capacity by a factor of 6. These values are very low compared to the value of 147 mAh/g observed for a similar xerogel nanocathode system studied by Patrissi and Martin [10]. Values for the geometric and the volumetric capacities were calculated using the dimensions and data above. Average values of approximately 20 μAh/cm^2 for the geometric capacity and 5 μAh/(cm^2 μm) for the volumetric capacity were obtained. Though smaller, these values compare favorably with Patrissi and Martin's values of 48 μAh/cm^3 and 9.6 μAh/(cm^2 μm) for a similar xerogel V_2O_5 system [20]. However, one must remember that all of these batteries were studied under ambient conditions where exposure to atmospheric water occurred. Future tests planned under inert atmosphere conditions should improve these results.

4. Conclusions

In summary, a technique has been developed for constructing microbatteries that could be used in micro- and nanosystems for a power source. Microbatteries with nanoscale features were made. Alumina filtration membranes having pores 200 nm in diameter served as the "jackets" to hold a PEO–lithium triflate electrolyte. Graphite particles that averaged 75 μm in diameter were placed on the membrane and covered numerous electrolyte-filled pores. An AFM cantilever was used to make contact with graphite particles, which served as the anodes for the microbatteries. The bottom of the pores had been filled with V_2O_5 xerogel making cathode structures having a circular surface area with a diameter of 200 nm. In some cases the V_2O_5 xerogel was filled with 35% carbon nanotubes making a nanocomposite cathode material. These microbatteries were charged and discharged proving that these small batteries could function. In effect microbatteries of numerous parallel nanocells were made. Future work will involve using smaller and smaller electrode particles until batteries with anodes and cathodes on the nanoscale are made making true nanobattery systems.

The charging studies were done under ambient conditions, which greatly hindered the observation of many of the beneficial effects associated with the nanoscale. The fact that electrodes on this scale typically show higher capacities, lower resistance, and lower susceptibility to slow electron-transfer kinetics, could not be investigated or taken advantage of because of the presence of water and oxygen during the cycling tests. The fact that studies have shown that polymer electrolytes confined in pores smaller than 400 nm have increased ion conduction [21] also could not be studied. This is the reason that techniques have been developed to conduct all future electrochemical tests including charge–discharge studies in the AFM under inert atmosphere conditions. This will allow the fundamental properties and benefits of such micro- and nanopower sources to be better understood.

Acknowledgements

The authors would like to acknowledge the Office of Naval Research and the National Science Foundation for funding this work. They would also like to thank Dr. Winton Cornell for assistance with the SEM and Robert Tipton and Ryan Leib for their help with the AFM studies.

References

[1] J.B. Bates, G.R. Gruzalski, M.J. Dudney, C.F. Lick, H.H. Yu, S.D. Jones, Solid State Technol. 36 (1993) 59.
[2] L.G. Salmon, R.A. Barksdale, B.R. Beachem, R.M. LaFollette, J.N. Harb, J.D. Holladay, P.H. Humble, in: Proceedings of the Solid-State Sensor and Actuator Workshop, Transducer Research Foundation Inc., Hilton Head, SC, 1998, pp. 338–341.
[3] K. Kinoshita, X. Song, J. Kim, M. Inaba, J. Kim, J. Power Sources 82 (1999) 170–175.
[4] S.V. Batty, T. Richardson, F.B. Dias, J.P. Voss, P.V. Wright, G. Ungar, Thin Solid Films 530 (1996) 284–285.
[5] Y. Zheng, F.B. Dias, P.V. Wright, G. Ungar, D. Bhatt, S.V. Batty, T. Richardson, Electrochim. Acta 43 (1998) 1633.
[6] J.H. Fendler, J. Dispersion, Sci. Technol. 20 (1999) 13.
[7] N.C. Li, C.J. Patrissi, G.G. Che, C.R. Martin, J. Electrochem. Soc. 147 (2000) 2044.
[8] N.C. Li, C.R. Martin, B. Scrosati, Electrochem. Solid State Lett. 3 (2000) 316.
[9] V.M. Cepad, J.C. Hulteen, G. Che, K.B. Jirage, B.B. Lakshmi, E.R. Fisher, C.R. Martin, Chem. Mater. 9 (1997) 1065.

[10] C.J. Patrissi, C.R. Martin, J. Electrochem. Soc. 146 (1999) 3176.
[11] G.G. Che, B.B. Lakshmi, E.R. Fisher, C.R. Martin, Nature 393 (1998) 346.
[12] Y.J. Park, K.S. Park, J.G. Kim, M.K. Kim, H.G. Kim, H.T. Chung, J. Power Sources 88 (2000) 250.
[13] Y.J. Park, J.G. Kim, M.K. Kim, H.G. Kim, H.T. Chung, Y. Park, J. Power Sources 87 (2000) 69.
[14] A. Levasseur, P. Vinatier, D. Gonbeau, Bull. Mater. Sci. 22 (1999) 607.
[15] K.S. Han, S. Tsurimoto, M. Yoshimura, Solid State Ion. 121 (1999) 229.
[16] Y. Park, J.G. Kim, M.K. Kim, H.T. Chung, W.S. Um, M.H. Kim, H.G. Kim, J. Power Sources 76 (1998) 41.
[17] R.A. Caruso, M. Antonietti, Chem. Mater. 13 (2001) 3272–3282.
[18] O. Pelletier, P. Davidson, C. Bourgaux, C. Coulon, S. Regnault, J. Livage, Langmuir 16 (2000) 5295–5303.
[19] V.G. Gavalas, R. Andrews, D. Bhattacharyya, L.G. Bachas, Nano Lett. 1 (2001) 719.
[20] C.J. Patrissi, C.R. Martin, J. Electrochem. Soc. 148 (2001) A1247.
[21] S. Vorrey, D. Teeters, Electrochim. Acta, in press.